Biophysical characterization and modeling of lung surfactant components

E. P. INGENITO,[1] L. MARK,[1] J. MORRIS,[2] F. F. ESPINOSA,[2] R. D. KAMM,[2] AND M. JOHNSON[2]
[1]*Division of Pulmonary and Critical Care Medicine, Brigham and Women's Hospital, Boston 02115; and* [2]*Department of Mechanical Engineering, Massachusetts Institute of Technology, Cambridge, Massachusetts 02139*

Ingenito, E. P., L. Mark, J. Morris, F. F. Espinosa, R. D. Kamm, and M. Johnson. Biophysical characterization and modeling of lung surfactant components. *J. Appl. Physiol.* 86(5): 1702–1714, 1999.—The present study characterizes the dynamic interfacial properties of calf lung surfactant (CLS) and samples reconstituted in a stepwise fashion from phospholipid (PL), hydrophobic apoprotein (HA), surfactant apoprotein A (SP-A), and neutral lipid fractions. Dipalmitoylphosphatidylcholine (DPPC), the major PL component of surfactant, was examined for comparison. Surface tension was measured over a range of oscillation frequencies (1–100 cycles/min) and bulk phase concentrations (0.01–1 mg/ml) by using a pulsating bubble surfactometer. Distinct differences in behavior were seen between samples. These differences were interpreted by using a previously validated model of surfactant adsorption kinetics that describes function in terms of *1*) adsorption rate coefficient (k_1), *2*) desorption rate coefficient (k_2), *3*) minimum equilibrium surface tension (γ^*), *4*) minimum surface tension at film collapse (γ_{min}), and *5*) change in surface tension with interfacial area for $\gamma < \gamma^*$ (m_2). Results show that DPPC and PL have k_1 and k_2 values several orders of magnitude lower than CLS. PL had a γ_{min} of 19–20 dyn/cm, significantly greater than CLS (nearly zero). Addition of the HA to PL restored dynamic interfacial behavior to nearly that of CLS. However, m_2 remained at a reduced level. Addition of the SP-A to PL + HA restored m_2 to a level similar to that of CLS. No further improvement in function occurred with the addition of the neutral lipid. These results support prior studies that show addition of HA to the PL markedly increases adsorption and film stability. However, SP-A is required to completely normalize dynamic behavior.

surface tension; dynamic; model; surfactometer

SURFACTANT is a complex mixture of phospholipids (PL), neutral lipids (NL), and proteins that imparts mechanical stability to alveolar structures by reducing surface tension. The PL fraction, the major component of lung surfactant by weight (80%), lowers surface tension at an air-liquid interface but does not possess adequate dynamic interfacial properties to function alone as an effective biological lung surfactant (20). Preparations of PLs with saturated acyl groups, such as dipalmitoylphosphatidylcholine (DPPC), achieve surface tensions of nearly zero during monolayer compression, but they respread poorly during subsequent film expansion and are lost from the interface during repeated cycling (10, 18). Addition of 10–30% PL that contains unsaturated acyl groups or addition of cholesterol improves film respreading but lowers the liquid-gel transition temperature of the lipid mixture, such that the films cannot support high surface pressures at body temperature (8, 30). As a result, such films collapse at 15–20 dyn/cm surface tension and would not be expected to confer stability to alveoli at low lung volumes (16).

Surfactant apoproteins (SP), which comprise only ~6–8% of lung surfactant by weight, appear to be critical for effective physiological function within the lung. In vitro studies have demonstrated that the addition of small amounts (1–2% by weight) of the low-molecular-weight surfactant hydrophobic apoproteins (HA), surfactant protein B (SP-B, 18,000) and surfactant protein C (SP-C, 3,500) dramatically increases the adsorption rate of surface-active material to an air-liquid interface compared with PLs alone (16, 20). Addition of HA or synthetic peptides of similar structure to PLs has also been shown to alter the surface film isotherm and to enhance respreading, such that near-zero surface tensions are achieved at body temperature during repeated cycling (3, 7). Surfactant protein A (SP-A), the most abundant of the SPs, increases adsorption of surface-active material to a small degree in isolation (20) and appears to play less of a direct role in determining interfacial properties than does HA. In the presence of calcium and the HAs, however, it significantly augments adsorption, such that PL-apoprotein mixtures behave as does native surfactant (9).

Wang et al. (32) systematically explored how different fractions of lung surfactant contribute to surfactant behavior by progressively reconstituting the hydrophobic fraction of lung surfactant and then comparing the transient surface-tension behavior of these samples with that exhibited by whole lung surfactant. Their findings, described in terms of minimum and maximum surface tension and a respreading parameter, included the observations that the PL fraction had an elevated minimum surface tension compared with either DPPC or calf lung surfactant (CLS) and that addition of the hydrophobic proteins was necessary for surface-tension behavior similar to that seen with native surfactant.

We look to extend these studies by completion of the reconstitution of lung surfactant, by addition back also of the hydrophilic component SP-A, by examination of the dynamic surface-tension behavior of these samples after they have reached steady state, and by interpretation of the difference in dynamic behavior between the surfactant fractions by using a model that characterizes a surfactant in terms of its biophysical properties. In the present study, we characterize the

The costs of publication of this article were defrayed in part by the payment of page charges. The article must therefore be hereby marked "*advertisement*" in accordance with 18 U.S.C. Section 1734 solely to indicate this fact.

dynamic behavior of lung surfactant fractions containing PL alone, PL + HA, PL + HA + SP-A, and PL + HA + SP-A + NL, and we compare their behaviors to those of native surfactant and DPPC. We confirmed the findings of Wang et al. (32) but also found that *1*) like the DPPC fraction, the PL fraction has a markedly decreased absorption rate compared with CLS, *2*) addition of NL did not significantly affect the dynamic interfacial properties of reconstituted surfactant already containing the full complement of SPs, and *3*) restoration of film compressibility (m_2) requires the presence of SP-A. Results suggest that both HA and SP-A are important for determining surfactant's overall function by affecting distinct biophysical properties of the lipid-protein mixture, whereas NL does not appear to play an important functional role when both HA and SP-A are present.

METHODS

Surfactant Isolation

Surfactant was isolated from fresh calf lungs within 3 h of tissue procurement. Lungs were lavaged with 4 liters of 0.15 M sodium chloride instilled under 25 cmH_2O pressure, and the return was collected by passive drainage. Cells were removed by low-speed centrifugation (250 *g* for 8 min at 4°C), and the supernatant was pooled. Crude surfactant was harvested by medium-speed centrifugation (40,000 *g* for 45 min at 4°C). Pellets were resuspended in 1–2 ml of sterile saline and were dispersed by injection through a 25-gauge needle. The crude surfactant was layered over 0.8 M sucrose in sodium chloride and was centrifuged at 30,000 *g* for 45 min at 4°C. The pellicles at the interface were aspirated, pooled, resuspended in saline, and ultracentrifuged (60,000 *g* for 30 min at 4°C). The resulting purified surfactant pellets were resuspended in 0.15 M NaCl that contained 0.2% sodium azide, divided into 1-ml aliquots that contained 10 mg/ml of PL each, and stored under nitrogen at −20°C. Samples stored in this fashion retained normal biophysical function and biochemical composition for up to 6 mo.

Preparation of Surfactant Fractions

The methodology used is a modified version of that previously developed by Hall et al. (7). One-milliliter aliquots of surfactant that containedg 10 mg of PL were injected through a 25-gauge needle into 45 ml of 1-butanol at room temperature. The samples were mixed slowly at room temperature for 30 min, and the aqueous soluble precipitate, containing predominantly SP-A and a small amount of serum proteins, was pelleted by centrifugation at 30,000 *g* for 30 min at 4°C. Pellets were dried under nitrogen at room temperature and were resuspended in 20 mM octylglucopyranoside by repeated injection through a 27-gauge needle. The solution was then ultracentrifuged for 1 h at 100,000 *g*, 4°C, and the pellet, which contained the purified SP-A fraction, was resuspended in 2–3 ml of 5 mM Tris buffer (pH 7.45) and dialyzed in a 2-liter Tris bath for 36 h, with three exchanges of buffer, with the use of a 12,000-molecular-weight-cutoff membrane (Spectra/Por no. 3; Spectrum). Purity was demonstrated by gel analysis. Total protein determinations were performed, and samples were aliquoted and stored at −20°C for subsequent use.

The butanol supernatant, which contained the hydrophobic fractions (including PLs, NLs, and the low-molecular-weight HAs SP-B and SP-C), was dried under vacuum and resuspended in $CHCl_3 \cdot MeOH$ (1:1 by volume; HPL grade, Fisher Scientific, Pittsburgh, PA). The sample, 2–3 ml in total volume, was applied to a 1.5 × 100-cm Sephadex LH-20 column (Pharmacia, Piscataway, NJ), and 1.5-ml fractions were eluted over 4–4.5 h at 4°C by using $CHCl_3 \cdot MeOH \cdot 0.1$ N HCl buffer (1:1:0.1 by volume). Fractions were brought to neutral pH by addition of 32 µl of 0.05 M HEPES buffer (pH 12). Protein, cholesterol, and PL assays were performed on 50-µl aliquots of each 1.5-ml fraction. Separation of protein, PL, and cholesterol-associated NL components was demonstrated, as previously reported (7), and fractions that contained each individual component were pooled and stored under nitrogen at −20°C for subsequent analysis.

Biochemical Analysis

Total protein determinations of surfactant samples that contained 150 µg of surfactant lipid were performed by amido black colorimetric assay and were compared with a bovine serum albumin standard curve prepared in 150 µg of aqueous sonicated DPPC (Sigma Chemical, St. Louis, MO) (12). PL content was determined by molybdenum blue P_i assay (1). Total cholesterol content of the NL fraction was determined by ferrous sulfate reduction assay (26).

The lipid composition of CLS and the fractions isolated by Sephadex chromatography were compared to verify that separation did not result in loss of any critical components. NL extraction of an aliquot of CLS was performed by cold acetone extraction (13). NL composition of CLS and pooled NL fractions from Sephadex chromatography were compared qualitatively by TLC. NL and CLS samples, each of which contained 250 µg of total cholesterol, were separated on silica G/H thin-layer plates (Fisher Scientific) by using a hexane-diethyl ether-formic acid (80:20:2) mobile phase (HPLC grade, Fisher Scientific) (14). Bands were detected by charring after sulfuric acid-potassium dichromate denaturation.

PL extraction of native surfactant was performed by using the method of Folch et al. (5). PL subtype composition of CLS and of pooled PL fractions obtained from Sephadex chromatography were compared after separation by TLC. From each sample, 400 µg of each sample, along with authentic PL standards, were spotted onto a Silica G/H TLC plate and were developed by using $CHCl_3 \cdot MeOH \cdot$ 2-propanol $\cdot H_2O \cdot$ triethylamine (42:12.6:9.8:35:35) mobile phase (HPLC-grade solvents; Fisher Scientific) (31). After separation, PL components were detected under low ultraviolet light after staining with atomized 1,3,5-diphenylhexatriene solution. Spots were scraped, and lipids were extracted into $CHCl_3 \cdot MeOH$ (50:50) by vigorous vortexing for 1 h at room temperature. Silica powder was removed by low-speed centrifugation, and the PL content of each component was determined by P_i assay.

SDS-PAGE was performed on pooled Sephadex fractions to verify the purity of SP-A and HA as well as the lack of protein cross contamination in the PL and NL fractions. All samples were run in duplicate, under reducing and nonreducing conditions, on 15% SDS polyacrylamide gels. Gels were stained with both Coomassie brilliant blue [0.1% in $MeOH \cdot AcOH \cdot H_2O$ (40:10:50), Sigma Chemical] and silver-stain reagent (Bio-Rad, Hercules, CA) to optimize detection of both SP-A and HA.

Surfactometry Sample Preparations

DPPC, PL, PL + HA, and PL + HA + NL samples were prepared from stock solutions in organic solvent aliquoted into glass test tubes, dried under vacuum, and resuspended

in 0.15 M NaCl, 5 mM $CaCl_2$. A homogeneous mixture was obtained by repeated injections and scraping by using a 1-ml syringe and a 25-gauge needle, respectively. Resuspended samples were vortexed for 15 min at room temperature under nitrogen. Each sample was transferred to a polypropylene microfuge tube and was sonicated twice for 30 s on ice. Aqueous SP-A was then added to appropriate samples, and additional vortexing was performed for 5 min at room temperature. Sample function was measured within 1 h of preparation.

Surfactometry Measurements

Equilibrium and dynamic surface-tension measurements were made by using a pulsating-bubble surfactometer (Electronetics, Amherst, NY) that was modified to use an external circulating-water-bath unit for temperature control and by installation of a stiffer spring into the sample clamp. These modifications minimized problems associated with drift of bubble size. To make measurements, we used a modification of the leak-free methodology previously described by Putz et al. (22). The technique employed in the present study utilized a plug that was fashioned from caulking putty to prevent leakage of surface-active material into the sample-chamber capillary tube during loading. We have found this approach to be much more reliable in prevention of tube wetting than was attempted occlusion of the capillary opening with a pin, as originally described.

Equilibrium surface-tension measurements were performed before any dynamic measurements were made under static conditions. Samples were loaded, as described above, and a bubble of 0.32-mm radius was formed by using the needle valve. Transfilm bubble pressure was then recorded as a function of time for a minimum of 15 min under nonoscillatory conditions at 1- to 2-min intervals until surface-tension changes were no longer observed to change as a function of time.

Dynamic measurements of surface tension as a function of surface area (assuming a spherical bubble shape) were made at bulk concentrations of 0.01, 0.1, and 1 mg/ml between 0.32- and 0.50-mm minimum-to-maximum bubble radius at oscillation frequencies of 1, 20, and 100 cycles/min. These modified dimensions were selected to better center the bubble on the sample chamber capillary tube during oscillations, which in turn reduces the occurrence of having bubbles break off during the compression phase of cycling. All recordings were made at 37°C until the system reached steady state (between 10 and 60 min, depending on the sample). Leakage of surface-active material up the capillary tube in the sample chamber was readily detected by an alteration in dynamic surface tension-surface area profiles and was confirmed by visual inspection of the sample-chamber capillary tube through the microscope objective (22). When leakage was detected, recordings were terminated, and samples were reanalyzed.

Data were obtained by using an area excursion of $\Delta A/A_{mean} \approx 85\%$ for all samples and for a few selected samples of $\Delta A/A_{mean} \approx 20\%$, where ΔA is surface-area excursion for one-half cycle and A_{mean} is mean surface area. For $\Delta A/A_{mean} \approx 85\%$, data presented are typical data drawn from four replicated experiments for CLS and from three experiments for the reconstituted fractions; for $\Delta A/A_{mean} \approx 20\%$, three experiments were conducted.

Computer Modeling

To understand which properties of the surfactant components were responsible for the difference in biophysical behavior seen between the surfactant fractions, we employed a previously developed model (19) that characterizes dynamic surfactant function in terms of five biophysical characteristics. This model differs from other models (e.g., Refs. 2 and 11) of surfactant transport in bubble surfactometers by allowing the interfacial surfactant concentration to dynamically rise higher than its maximum equilibrium value and by consideration of the phase changes in surfactant that occur at these high interfacial concentrations. We first briefly describe the model and then discuss the use of this model to interpret our results from the different surfactant fractions.

Explanation of the model. This model characterizes surfactant transport to and from the interface in terms of three distinct surface concentration regimes (see Fig. 1).

REGIME 1. Surface concentration (Γ, measured in moles of surfactant per cm^2 surface area) is less than the maximum equilibrium surface concentration (Γ^*) that can be achieved as bulk-phase concentration (C) is increased (Fig. 1, *segment F-C*). In this regime, adsorption and desorption to and from the interface are assumed to occur according to the Langmuir relationship

$$dM/dt = A[k_1C(\Gamma^* - \Gamma) - k_2\Gamma] \quad (1)$$

where t is time, k_1 is the adsorption coefficient, k_2 is the desorption coefficient, A is the interfacial area, and M is ΓA (the amount of surfactant in the interface). Surface tension (γ) is related to surface concentration through the static isotherm relationship which is assumed to decrease linearly with increasing surface concentration Γ, such that $\gamma = 70$ dyn/cm when $\Gamma/\Gamma^* = 0$, and $\gamma = \gamma^*$ when $\Gamma/\Gamma^* = 1$. This relationship defines the isotherm slope $m_1 = -d\gamma/d(\Gamma/\Gamma^*)$.

REGIME 2. Surface concentration Γ is greater than Γ^* but less than the maximum concentration (Γ_{max}) that can be achieved during lateral compression of surface-active material at the interface (Fig. 1, *segments C-D* and *E-F*). In this regime, the surfactant is modeled as insoluble, i.e., it does not exchange surface-active material with the bulk phase. The relationship between γ and Γ/Γ^* in this regime decreases

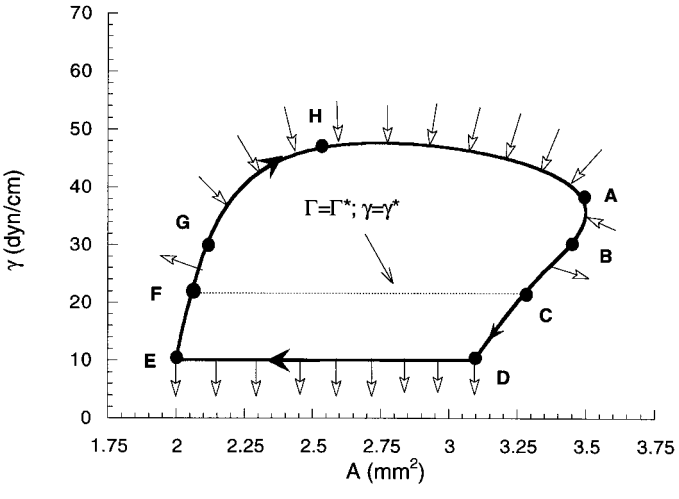

Fig. 1. Schematic of surface tension (γ) vs. bubble area (A) loop demonstrating surfactant transfer mechanisms for each loop segment. Γ, Interfacial surfactant concentration. Loop direction is clockwise. Kinetic adsorption (between *G* and *B* along *top* of loop) or desorption (*segments F-G* and *B-C*) for $\gamma > \gamma^*$ (*regime 1*); insoluble monolayer for $\gamma_{min} < \gamma < \gamma^*$ (*segments C-D* and *E-F*) (*regime 2*); and squeeze out as the area is lowered beyond the point where γ_{min} is reached (between *D* and *E*) (*regime 3*) are shown. Inward and outward arrows represent adsorption, desorption, and squeeze out of surfactant by the monolayer.

linearly with a slope ($-m_2$) which is distinct from m_1. It is important to note that this region cannot be characterized from static measurements of surfactant. The film must undergo external dynamic compression to reach these low surface tensions. This critical regime of surfactant function has not been included in previous models of dynamic surfactant function.

REGIME 3. Γ is equal to Γ_{max} (Fig. 1, *segment D-E*). Surfactant molecules are packed as tightly as possible in the interface, and surface concentration cannot increase further. Surface tension reaches its minimum value (γ_{min}) at this point and remains constant as surface area is further decreased by film compression. Any further compression leads to material being lost from the surface to the bulk by squeeze out or film collapse.

Estimation of model parameters. The model is characterized by five parameters: the surfactant adsorption (k_1) and desorption (k_2) rate constants in *regime 1*, the minimum equilibrium surface tension (γ^*), the slope m_2, and the minimum achievable surface tension during film compression (γ_{min}). Note that m_1 is entirely determined by γ^*. These parameters can be estimated from equilibrium and dynamic surface tension measurements made by using the pulsating-bubble surfactometer. Our goal in the present study was to determine which of these biophysical parameters are responsible for the differences seen between samples reconstituted from purified surfactant fractions and CLS native surfactant. To do this, we first estimated the values of these parameters for native surfactant and then systematically varied these parameters to determine what changes were necessary to qualitatively produce dynamic profiles similar to those seen in the reconstituted samples.

For native surfactant, we determined γ^* as the lowest equilibrium surface tension measured as bulk concentration was increased up to 5 mg/ml. The γ_{min} was determined as the lowest surface tension achieved during dynamic film compression at the highest bulk concentration (1 mg/ml) studied. The isotherm slope m_2 was determined by using the surface tension vs. surface area slope ($d\gamma/dA$) in the insoluble regime during dynamic oscillations (Fig. 1, *segment C-D*) as surface tension was decreased from γ^* to γ_{min} during film compression for samples at high bulk concentration (1 mg/ml). To find m_2, we divided this slope by $d(\Gamma/\Gamma^*)/dA = (-\Gamma/\Gamma^*)/A$ (the insoluble regime).

Both k_1 and m_2 dictate the behavior of the model at a high concentration. Once m_2 has been characterized, values for k_1 can be determined independently by matching model curves to the dynamic data. As a criterion for determining m_2, we matched the surface area at which the surface tension reaches its minimum value during dynamic compression (*point D* in Fig. 1). At low concentrations, the sole determinant of model function is k_1/k_2 because, at these concentrations, the insoluble region is never reached and, therefore, m_2 plays no role. We selected the minimum surface tension achieved during dynamic cycling as the characteristic parameter for matching each low-concentration profile.

RESULTS

Biochemical Composition of CLS

CLS used in the present study was found to be 92.5 ± 0.1 (SD) % lipid and 7.5 ± 0.1% protein by weight ($n = 3$ samples). The lipid fraction was composed of 91 ± 2% PL and 9 ± 1% cholesterol ($n = 3$ samples). Smaller amounts of noncholesterol NLs were present as identified by TLC, but they were not quantified in our analysis. These results are consistent with previously published data (32). PL subtype analysis performed on organic extracts of CLS and followed by TLC separation was similar to that previously reported (32). Results are summarized as follows ($n = 3$; in %): 80.8 ± 0.2 phosphatidylcholine (PC), 7.7 ± 0.4 phosphatidylglycerol (PG), 5.5 ± 0.1 phosphatidylserine-phosphatidylinositol (PS/PI), 2.0 ± 0.3 phosphatidylethanolamine (PE), 2.0 ± 0.2 sphingomyelin (SM), and 2.0 ± 0.1 cardiolipin (CL).

Composition of Surfactant Fractions

Of total PL, 55% was recovered after separation (mean recovery from 2 separate purifications of 61 and 49%). The purity of each pooled fraction obtained from column chromatography (LH-20) was assessed by protein, cholesterol, and PL assay. The hydrophobic fraction contained 89% HAs, 5.5% PLs, and 5.5% cholesterol. The PL fraction contained 99.7% PLs and 0.3% cholesterol. The cholesterol fraction contained 91% cholesterol and 9% PLs.

SDS-PAGE was performed to further assess the composition of each fraction. Results are shown in Fig. 2. No detectable SP-A or serum proteins were observed in HA fractions by silver-Coomassie brilliant blue staining. The SP-A fraction contained no detectable HA or serum. PL and cholesterol fractions contained no significant amounts of either major SP components.

Pooled NL components, separated by TLC by using hexane-diethyl ether-formic acid mobile phase, were detected by acid denaturation and charring as previously described. Qualitative analysis demonstrated that cholesterol was the major component present in this fraction, but cholesterol ester, dipalmitin, tripalmitin, a very small amount of free fatty acid, and a minor PL component were also present. NL composition after LH-20 separation was similar to that determined for NL-acetone extracts isolated from native surfactant.

PL composition after LH-20 separation, as determined by TLC, was nearly identical to that observed in CLS after Folch extraction. PL composition of CLS was as follows ($n = 3$; in %): 80.8 ± 1.9 PC, 7.7 ± 0.8 PG, 5.5 ± 1.1 PS/PI, 2.0 ± 0.3 PE, 2.0 ± 0.3 SM, and 2.0 ± 0.4 CL. Composition of PL fraction was found to be ($n = 4$; in %): 79.5 ± 2.1 PC, 6.7 ± 1.3 PG, 6.6 ± 1.0 PS/PI, 2.5 ± 0.4 PE, 2.8 ± 0.5 SM, and 1.7 ± 0.3 CL.

Characterization of Biophysical Properties by Surfactometry

Significant differences were seen between the dynamic behavior of CLS and that of the surfactant fractions. We begin with a detailed description of CLS, as this is the baseline to which the other samples are compared. Figure 3, *A-C*, shows typical experimental results for CLS measured at 20 cycles/min [a complete data set for CLS and the other surfactant fractions can be found in Morris (15)]. At 1 mg/ml, CLS reached a minimum surface tension of <1 dyn/cm after a relatively small degree of compression for all three oscillation frequencies examined. The maximum surface ten-

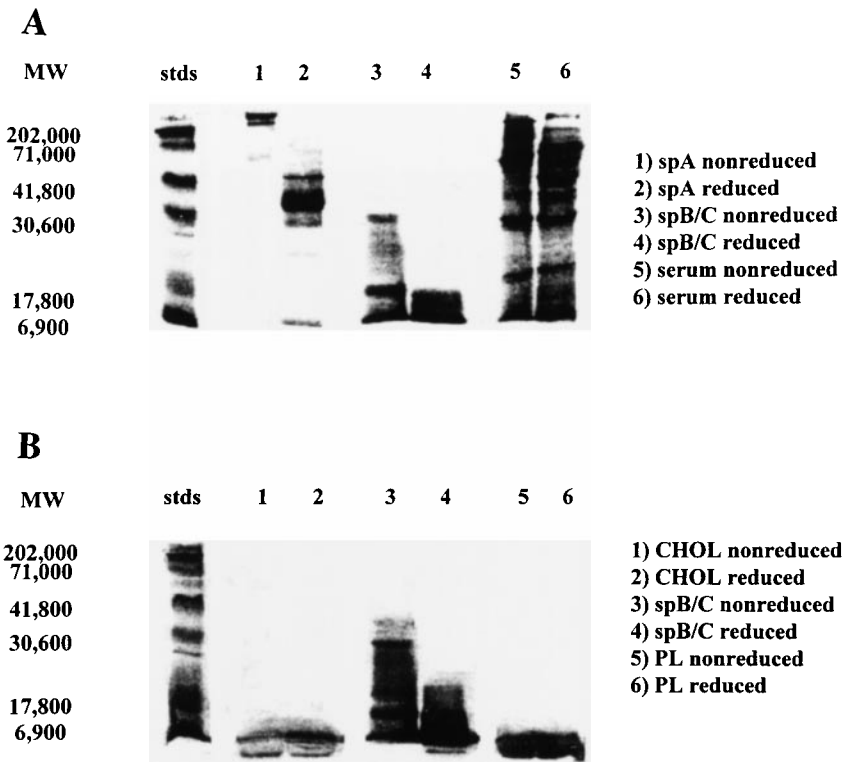

Fig. 2. SDS-PAGE analysis of both hydrophobic apoprotein (HA) and surfactant apoprotein A (SP-A) fractions (*A*) and hydrophobic pooled fractions (*B*). Hydrophobic fractions were separated by 15% SDS-PAGE. HA and SP-A fractions were separated by 12% SDS-PAGE. Each gel was stained with both Coomassie blue and silver stain to maximize detection of components; 50 μg of phospholipid (PL) and cholesterol (Chol), and 2 μg of hydrophobic proteins were examined under both reducing and nonreducing conditions, and 5 μg of each protein fraction were analyzed in similar fashion. SP-B and SP-C, surfactant proteins B and C, respectively; stds, standards; MW, mol. wt. *Lanes 1–6* are identified in *right* column.

sion varied with frequency from ~30 dyn/cm at 1 cycle/min and increased to ~40 dyn/cm at 100 cycles/min. Very significant hysteresis was seen at all frequencies.

At 0.1 mg/ml, the minimum surface tension typically reached values <5 dyn/cm, but it did not always reach the very-low-surface-tension values seen with 1 mg/ml. Furthermore, greater compression was necessary to reach minimum surface tension (typically 50%). Maximum surface tension was similar to that of 1 mg/ml at 1 cycle/min, but it increased to >60 dyn/cm at the higher frequencies. With a further reduction in bulk concentration to 0.01 mg/ml, minimum surface tension rose to 20 dyn/cm, and maximum surface tension during film expansion was always >60 dyn/cm. Hysteresis was reduced at 0.1 and 0.01 mg/ml compared with 1 mg/ml.

DPPC, the major PL component of lung surfactant, demonstrated markedly different interfacial properties (Fig. 4, *A-C*). Whereas DPPC achieved minimum surface tension near 0 dyn/cm (similar to CLS), >50% film compression was required to reach this minimum. Furthermore, hysteresis in DPPC samples is markedly reduced at 1 and 0.1 mg/ml from that seen in CLS. Another notable difference was that the maximum surface tension was >50 dyn/cm (usually >60 dyn/cm) for all bulk concentrations and frequencies examined.

Figure 4, *D-F*, summarizes the dynamic interfacial properties of the purified PL fraction, which constituted 84% of surfactant by weight. In contrast to CLS and DPPC, PL reached a minimum surface tension during film compression of only 20 dyn/cm at 1 mg/ml bulk concentration. Roughly 50% film compression was required to achieve this minimum surface tension. Maximum surface tension was similar to that of DPPC, but the hysteresis was significantly greater for all conditions examined.

The addition of HAs (3% by weight) to PL had a dramatic effect on interfacial properties and restored much of the dynamic behavior of native surfactant (Fig. 5, *B* and *C*). Film stability during compression was markedly increased, such that minimum surface tensions close to 0 dyn/cm were achieved at a concentration of 1 mg/ml, although greater film compression than in CLS samples was required to achieve these minimums at all frequencies examined (e.g., Fig. 5*A*). PL + HA behaved similarly to CLS at 0.1 and 0.01 mg/ml for all three frequencies.

Addition of SP-A to PL + HA at physiological concentrations restored the dynamic performance to nearly that of CLS (Fig. 5, *D-F*). SP-A decreased the film compression required to achieve surface tensions <1 dyn/cm to values similar to, but slightly higher than, that of CLS. The dynamic behavior of the samples was similar to CLS with respect to minimum and maximum surface tensions and hysteresis at all concentrations and frequencies considered.

Addition of NLs to PL + HA + SP-A had little further effect on steady-state behavior. Figure 3, *D-F*, shows that this reconstituted surfactant had biophysical properties very similar to those of native surfactant (Fig. 3, *A-C*).

Estimation of Model Parameters for Native Surfactant

Our best fit to the dynamic profiles for native surfactant yielded parameters values of $\gamma^* = 22.2$ dyn/cm,

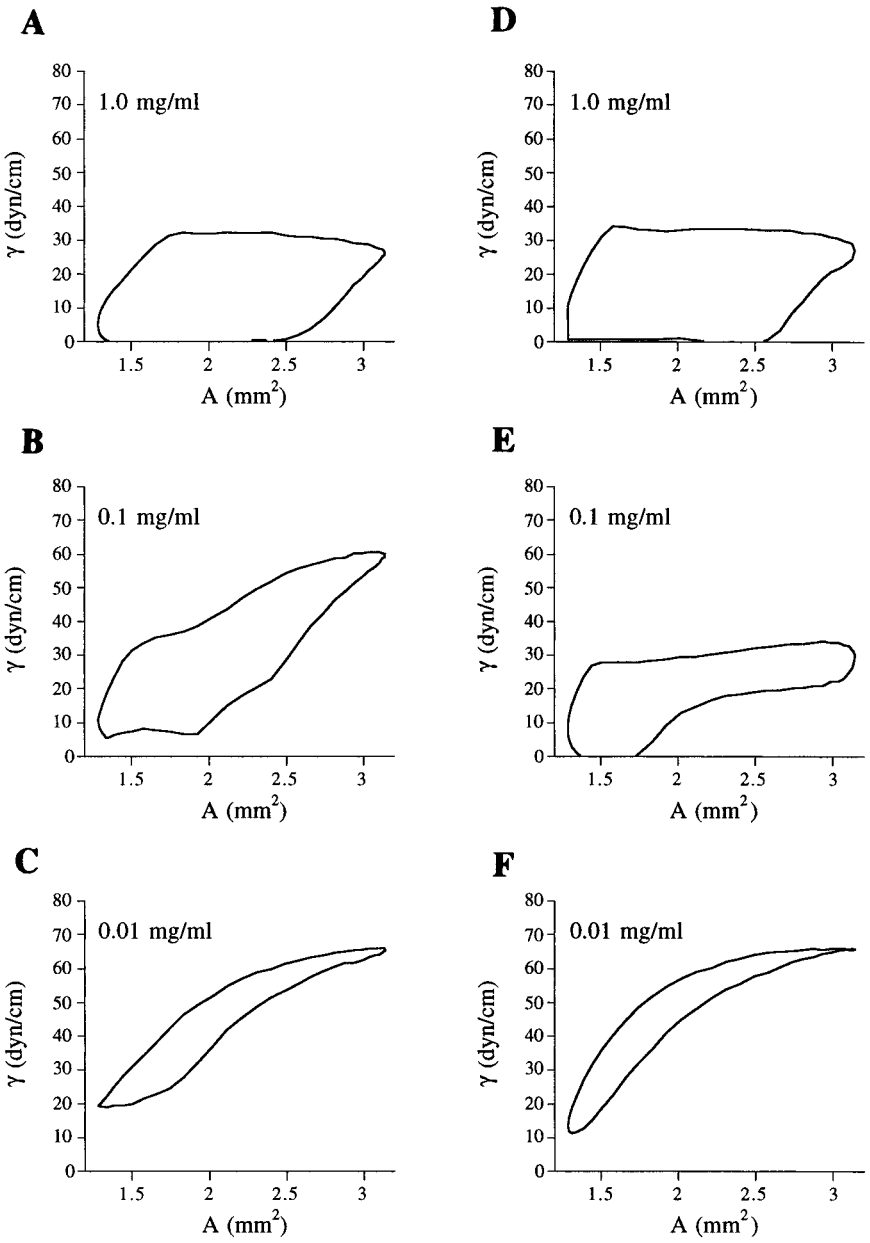

Fig. 3. Typical loops of surface tension vs. interfacial area for calf lung surfactant (CLS) (*A-C*) or reconstituted surfactant containing PL + HA + SP-A + neutral lipid (NL) fractions (*D-F*), in 5 mM $CaCl_2$ and 0.15 M NaCl, as measured during dynamic oscillations by pulsating-bubble surfactometry at a frequency of 20 cycles/min at bulk concentrations of 0.1–1 mg/ml.

γ_{min} = 1 dyn/cm, m_2 = 140 dyn/cm, $k_1 = 6 \times 10^5$ ml·g^{-1}·min^{-1}, and $k_1/k_2 = 1.2 \times 10^5$ ml/g. Model predictions made by using these parameter values are shown in Fig. 6, *A-C*. Compared with Fig. 3, *A-C* (native surfactant), the agreement is seen to be very good, except for the predictions of maximum surface tensions, a weakness of the model, as previously discussed (19).

One of the features of our data and model predictions concerning native surfactant is notable and requires further comment: the effect of bulk concentration on the results. The results shown in Fig. 3, *A-C*, are for bulk concentrations of surfactant many orders of magnitude higher than the critical micellar concentration (CMC) of DPPC (3.5×10^{-7} mg/ml) (29). Thus, at first, it may seem surprising that any difference is seen between the results for different bulk concentrations (note that this is also true for the DPPC experiments, Fig. 4, *A-C*). The CMC is the concentration at which micelles are thermodynamically favored in solution over individual molecules in a solution without an air-water interface. If an interface is present, it gives the molecules a third thermodynamic option, namely, to occupy the interface. There is no reason to expect that the bulk concentration that leads to a saturation of the interface (CBC = $100 \cdot k_2/k_1$, defined as that bulk concentration at which $\Gamma = 0.99\ \Gamma^*$, which for CLS is ~0.8 mg/ml) should be the same as the CMC, because the free energy of a surfactant molecule at an interface is not necessarily the same as the free energy of a surfactant molecule in a micelle. Apparently, DPPC molecules have such a preference for an interface that the CBC value for this surfactant is substantially greater than the CMC.

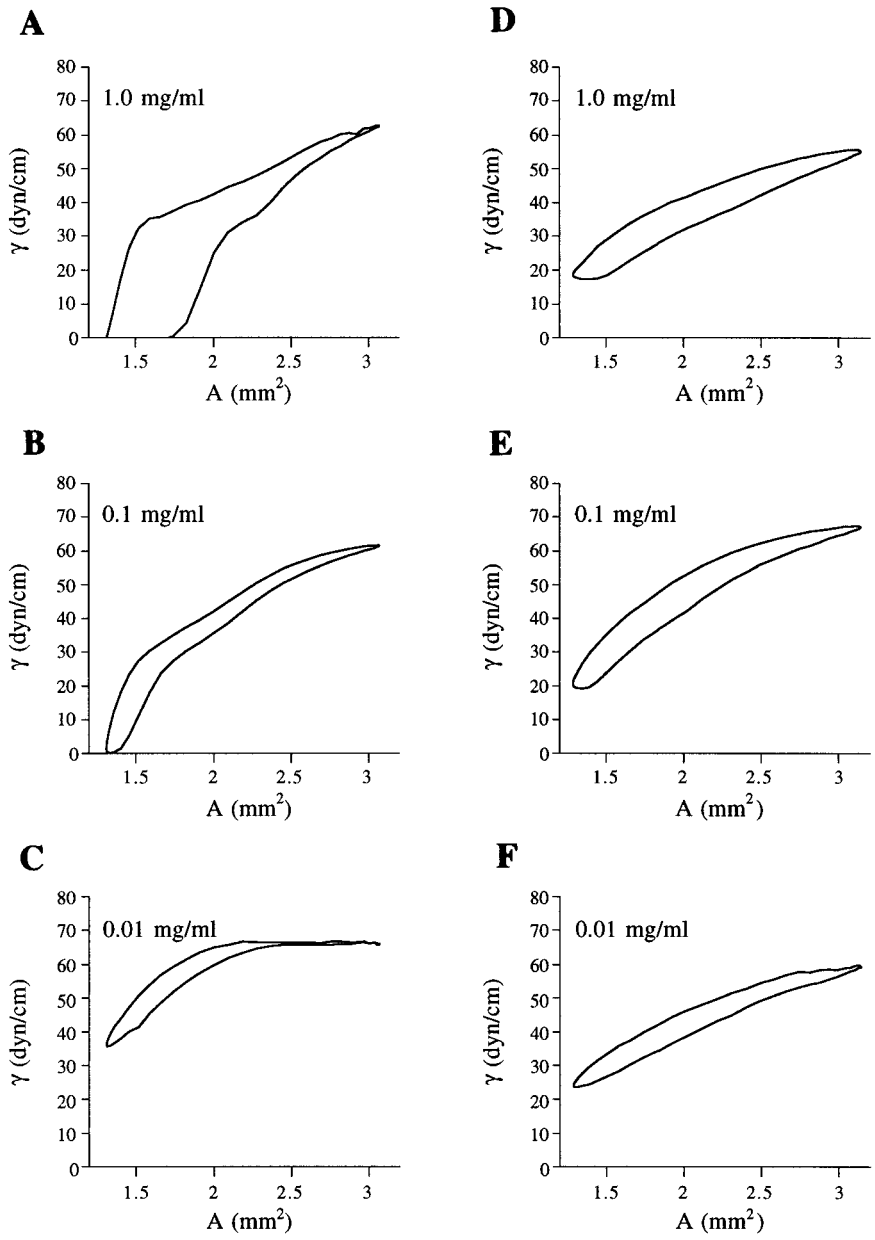

Fig. 4. Typical loops of surface tension vs. interfacial area for dipalmitoylphosphatidylcholine (DPPC; *A-C*) or the purified PL fraction (*D-F*), in 5 mM $CaCl_2$ and 0.15 M NaCl, as measured during dynamic oscillations by pulsating-bubble surfactometry at a frequency of 20 cycles/min at bulk concentrations of 0.1–1 mg/ml.

Effect of Parameter Variation on Predicted Surfactant Dynamic Behavior

We investigated three scenarios of how these parameters might change, thus leading to altered surfactant biophysical behavior: *1*) a decreased rate of surfactant adsorption to and desorption from the interface, *2*) an increased surface tension at which squeeze out or collapse occurs, and *3*) an increase in the level of compression required to reduce surface tension in *regime 2*. In the first scenario, we decreased k_1 while keeping the ratio of k_1/k_2 constant. The results are shown in Fig. 6, *D-F*, for a 10-fold (dashed line) or 100-fold (solid line) reduction in transport rate. Figure 7, *A-C*, shows the effect of increasing γ_{min} from 0 to 22.2 dyn/cm, whereas Fig. 7, *D-F*, shows the combination of a reduction in surfactant transport rate (*scenario 1*) with an increased γ_{min} (*scenario 2*). Figure 8, *A-C*, shows the effect of decreasing m_2 by twofold (solid line) and fourfold (dashed line).

Comparison of Fig. 6, *D-F*, with Fig. 4, *A-C*, allows us to conclude that DPPC adsorbs and desorbs to the interface much more slowly than does CLS, as previously reported (7, 20). Our computer model indicates that DPPC has values of k_1 and k_2 that are roughly two orders of magnitude lower than does CLS. Note that this indicates that the increased compression required to decrease the surface tension of DPPC to <1 dyn/cm, compared with CLS (Fig. 4*A* vs. Fig. 3*A*), can be entirely explained as a change in k_1 rather than involving other parameters (in particular m_2).

In contrast, the PL fraction of native surfactant shows a much different behavior (Fig. 4, *D-F*). It is apparent that the surface tension at which squeeze out or collapse occurs (Fig. 1, *segment D-E*) is much higher

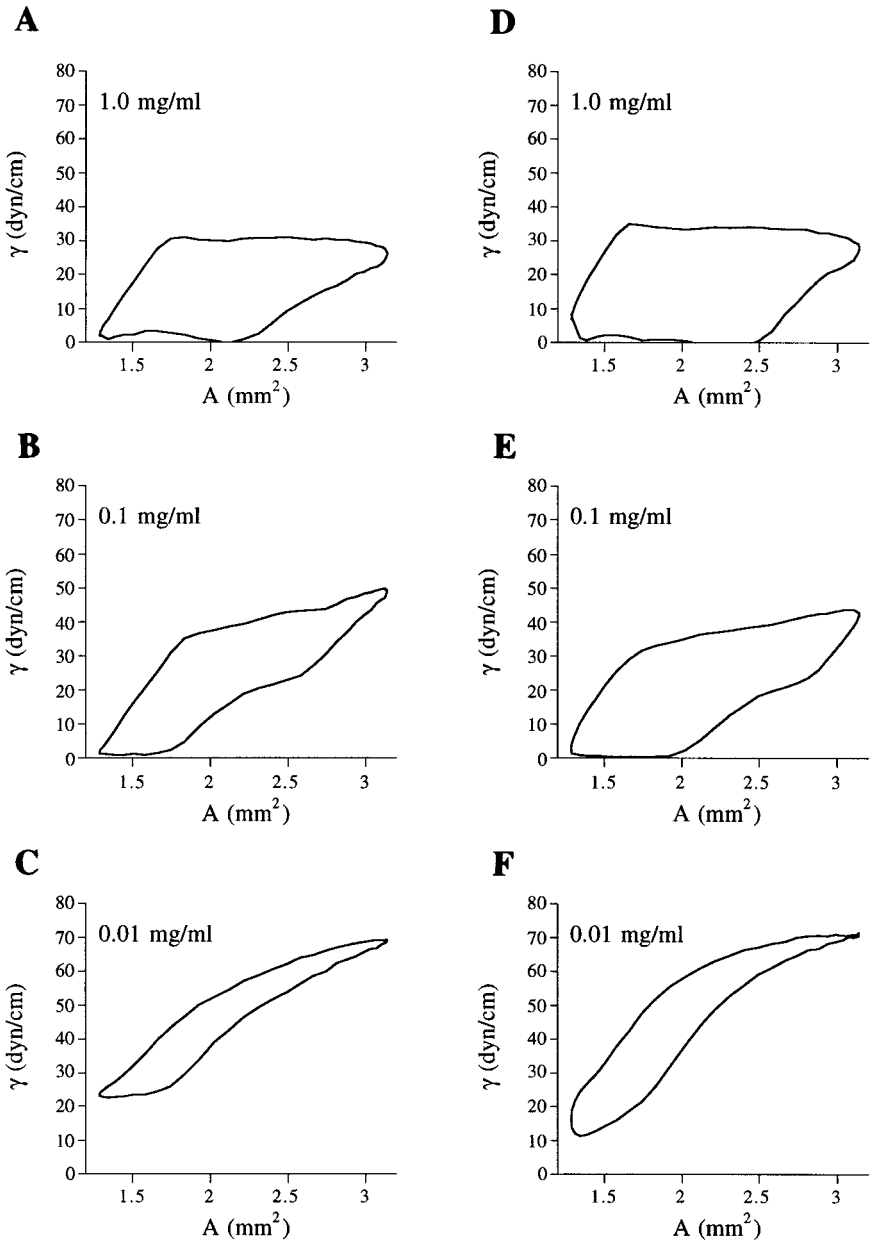

Fig. 5. Typical loops of surface tension vs. interfacial area for PL + HA fraction (*A-C*) or PL + HA + SP-A fraction (*D-F*), in 5 mM $CaCl_2$ and 0.15 M NaCl, as measured during dynamic oscillations by pulsating-bubble surfactometry at a frequency of 20 cycles/min at bulk concentrations of 0.1–1 mg/ml.

than in CLS. However, the model indicates that a simple increase in γ_{min} to 20 dyn/cm (Fig. 7, *A-C*) does not entirely account for the altered dynamic profiles in PL samples. It is necessary to lower k_1 and k_2 (to a similar extent as that seen with DPPC) as well as to increase γ_{min} to produce dynamic profiles that are similar to those seen in PL samples (Fig. 4, *D-F*).

Finally, we investigated the predicted effects of decreasing m_2. As shown in Fig. 8, *A-C*, decreasing m_2, first by twofold and then by fourfold, had two effects on dynamic behavior compared with the baseline case: *1*) it caused an increase in the amount of compression necessary to reach a minimum surface tension, and *2*) it caused a decrease in maximum surface tension reached. This behavior is very similar to that seen with the PL + HA mixtures (Fig. 5, *A-C*), the data for which are best fit by the twofold reduction in m_2. Note that the addition of SP-A increased m_2 and restored dynamic behavior similar to that of CLS.

Comparison of computer-model predictions with experimental data indicates that both DPPC and PL fractions have a greatly increased resistance to transport to the interface, as reflected in a low k_1 relative to CLS. The PL fraction is further deficient in that it squeezes out of the interface or collapses at much lower surface pressures. Addition of the HAs restores these biophysical properties, but m_2 is reduced compared with CLS, and m_2 likely relates to the packing efficiency of the film at high surface pressures. Addition of SP-A restores this property to the reconstituted surfactant.

Behavior of the System for Physiological Values of ΔA/A

On the basis of the findings described in the previous section, we were curious as to whether the reduction of m_2 in the PL + HA fraction, which appeared to be due to lack of SP-A, might be physiologically significant. Our

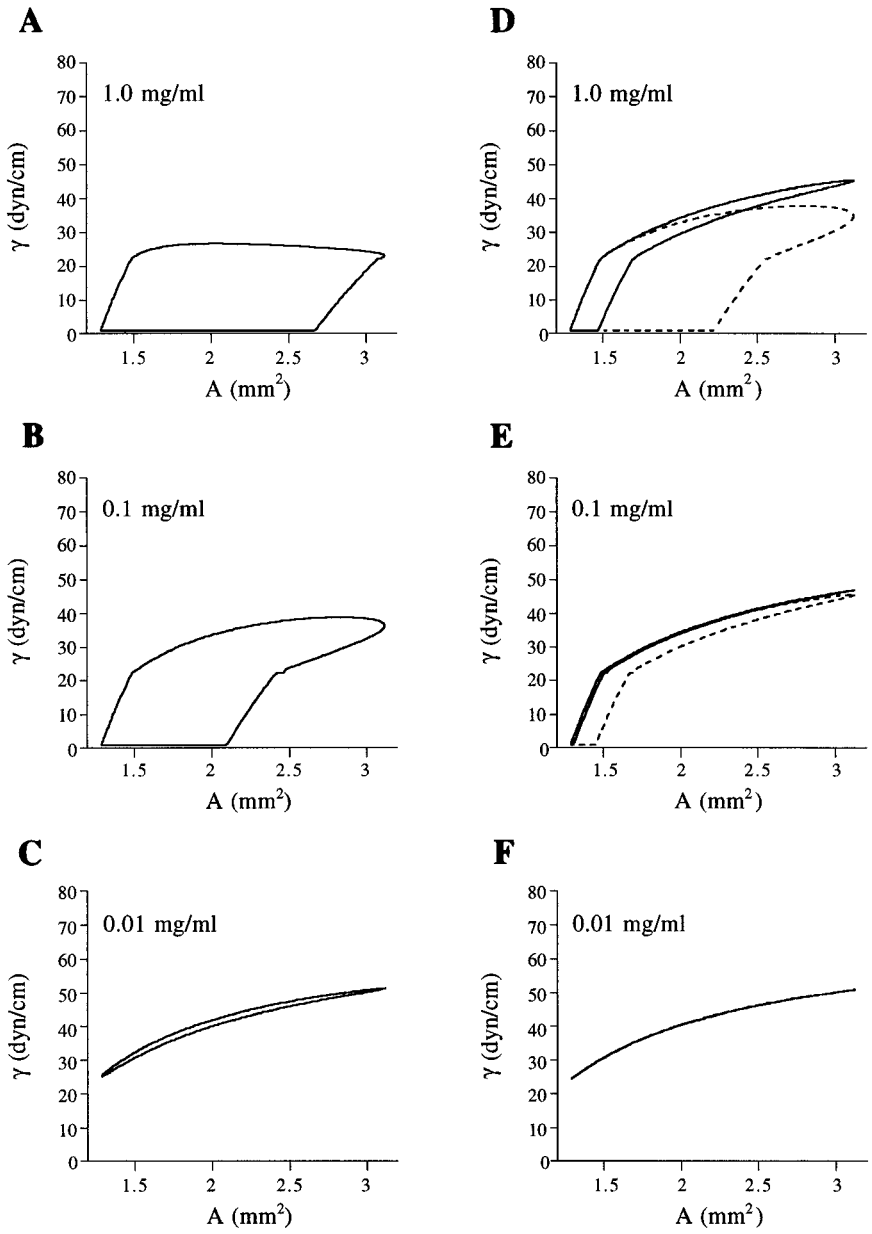

Fig. 6. Prediction of computer model for dynamic surface tension vs. interfacial area for baseline case of CLS (*A-C*), and additional simulations showing how these loops are affected by a 10-fold (dashed line) or 100-fold (solid line) reduction of k_1, with k_1/k_2 and all other parameters kept constant (*D-F*). Frequency is 20 cycles/min at bulk concentrations of 0.1–1 mg/ml.

computer model predicted that a significant and functionally relevant difference would be seen between the CLS and PL + HA for a $\Delta A/A$ of 20% [in the physiological range (17)] (Fig. 9*A*). To confirm this, dynamic surface-tension measurements were made at small values of $\Delta A/A$, and profiles for these fractions (Fig. 9*B*) were found to be very similar to those predicted by the computer model.

DISCUSSION

In this study, we have examined the dynamic surface tension characteristics of CLS and its major constituents with the goal of *1*) determination of the functional role of each component and *2*) determination of whether surfactant reconstituted from purified, biochemically defined components exhibits interfacial properties similar to those of native surfactant. Our fractionation of CLS yielded a surfactant profile (67% PC, 16% other surfactant PL, 9% NL, 3% surfactant HAs, and 5% SP-A) similar to that reported by other investigators (16, 32). Our measurements of surface tension of CLS and its fractions, combined with modeling studies, indicate that each of the fractions, with the exception of the NL fraction, is important in the determination of the biophysical properties of CLS, and, furthermore, that reconstituted lung surfactant behaves nearly identically to CLS.

Previous studies that have examined the interfacial properties of artificial surfactant mixtures and purified native surfactant fractions have shown that PLs alone lack the ability to function effectively as biological surfactants (8, 16, 28, 32). We found that DPPC, the major PL constituent of surfactant, can reach surface tensions of <2 dyn/cm at steady state during oscillations at 1, 20, and 100 cycles/min (Fig. 4, *A-C*). However, it had an adsorption rate k_1 several orders of

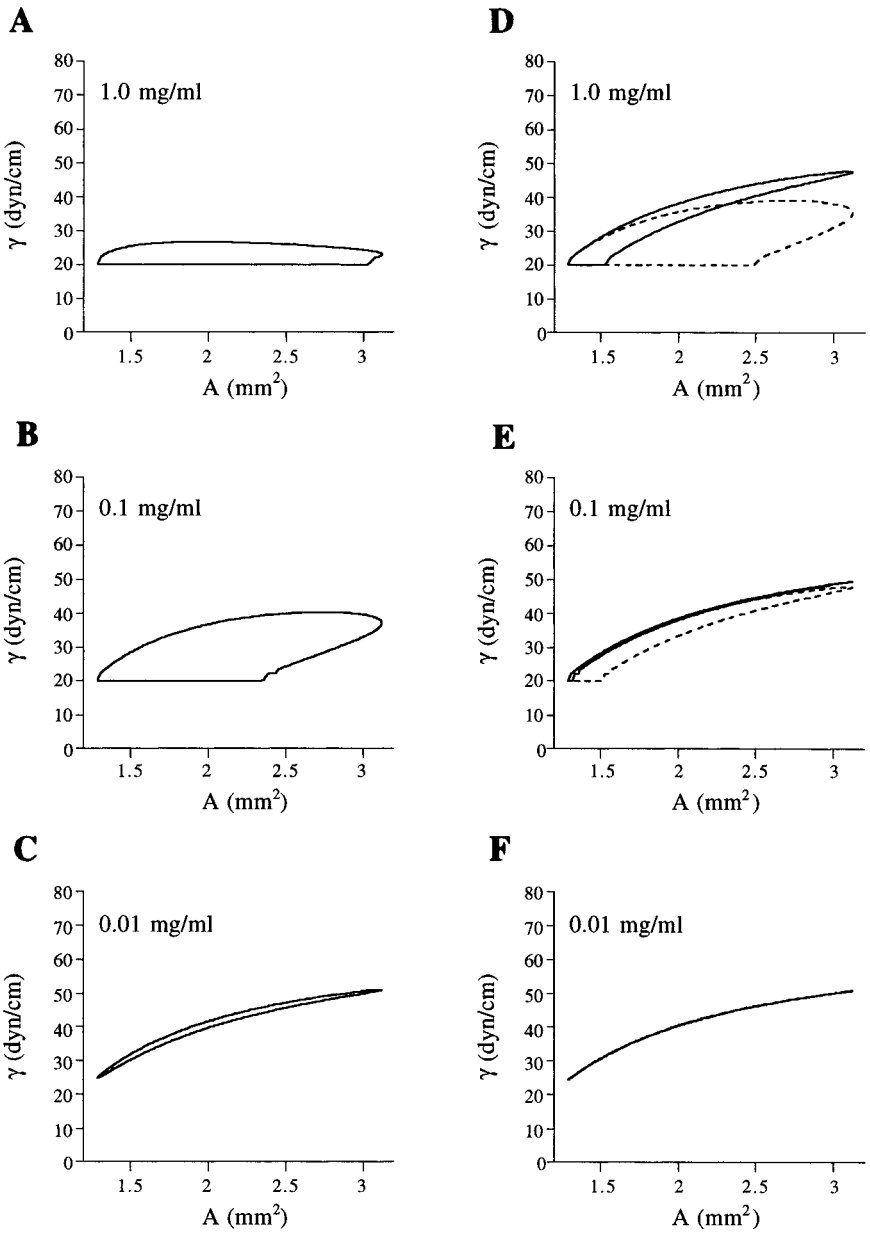

Fig. 7. *A-C*: prediction of computer model for dynamic surface tension vs. interfacial area for effects of increasing γ_{min} to 20 dyn/cm. *D-F*: increasing γ_{min} to 20 dyn/cm and decreasing k_1 by 10-fold (dashed line) or 100-fold (solid line) while keeping k_1/k_2 and all other parameters constant. Frequency is 20 cycles/min at bulk concentrations of 0.1–1 mg/ml.

magnitude lower than did CLS (Fig. 6, *D-F*), which would preclude it from being biologically effective in the lung during normal respiration (16).

Although composed largely of DPPC, the PL fraction of native surfactant behaved quite differently from pure DPPC (Fig. 4, *D-F*). The adsorption rate was similar to that of DPPC and much slower than that of biologically active native surfactant (Fig. 7, *D-F*). However, PL was significantly less stable at high surface pressures than were both DPPC and CLS, as demonstrated by film collapse at 21–24 dyn/cm. This observation is similar to that previously reported by Wang et al. (32) and may relate to the heterogeneous acyl chain composition of the PL fraction. Both chain length and degree of unsaturation have been shown to influence the rate of respreading after extrusion of PL components from the air-liquid interface and the critical transition temperature at which a lipid gel melts to assume a less stable, liquid conformation (4, 6, 8, 10).

Addition of the HAs had two important effects on surface film function. First, as reported by others (9, 24), these components restored the adsorption rate k_1 to a value similar to that of CLS. Second, HA imparted stability to the PL fraction during film compression, such that minimum surface tensions <1 dyn/cm could be achieved at physiological temperatures (32). PL + HA mixtures reached minimum and maximum surface tensions similar to those of native surfactant at all frequencies and concentrations tested. However, m_2 was significantly less than that of CLS, such that greater film compression (40–45%) was required to achieve minimum surface tensions of <1 dyn/cm.

The addition of SP-A to PL + HA increased the m_2 slope to be nearly equal to that of CLS. PL + HA + SP-A

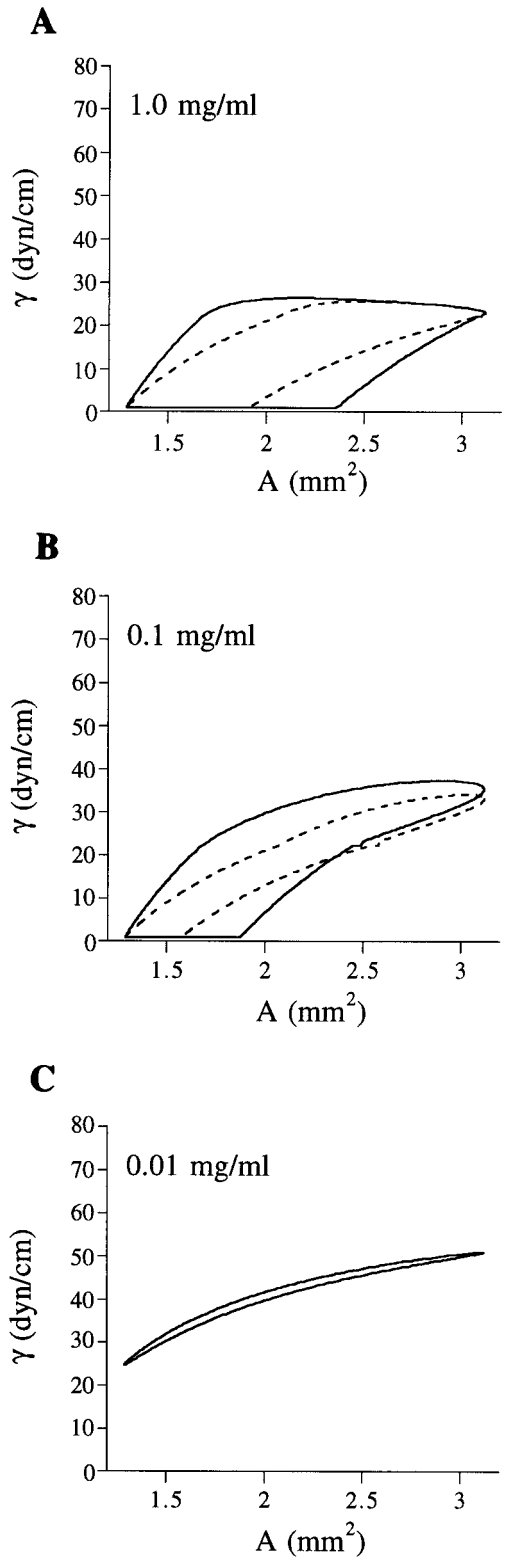

Fig. 8. Prediction of computer model for dynamic surface tension vs. interfacial area for effects of decreasing change in surface tension with interfacial area for $\gamma < \gamma^*$ (m_2) by 2-fold (solid line) or 4-fold (dashed line) while keeping other parameters constant. Frequency is 20 cycles/min at bulk concentrations of 0.1–1 mg/ml.

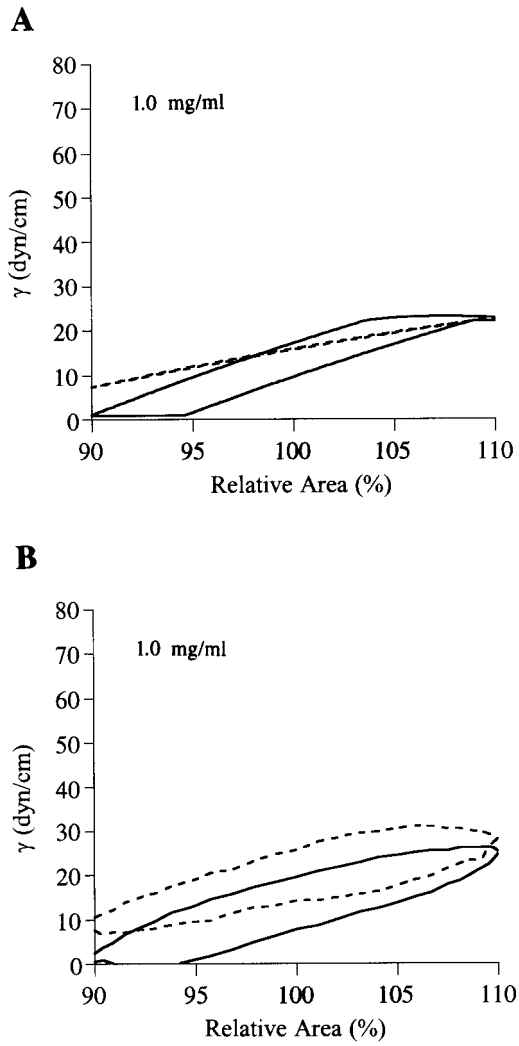

Fig. 9. Surface tension vs. relative surface-area profiles of simulated tidal breathing area excursions ($\Delta A/A_{mean}$ = 20%) for theoretical prediction for baseline case of CLS (solid line, *A*) and for reducing m_2 by 2-fold (dashed line, *A*). *B*: typical experimental data at same conditions (1 mg/ml and 20 cycles/min) for CLS (solid line) and PL + HA (dashed line).

mixtures functioned similarly to CLS in all respects at all frequencies and bulk phase concentrations studied. The addition of NL to the PL + HA + SP-A mixture had little additional effect on interfacial properties under steady-state conditions.

The biophysical changes that occur in response to stepwise reconstitution of surfactant appear to relate to specific molecular changes in film organization that are caused by each of the apoprotein components. Electron microscopy studies and resonance energy transfer fluorescence studies suggest that HA promotes dissolution of large micelle structures and fusion of micellar contents and thus makes lipid mixtures behave more homogeneously in an aqueous environment (21, 23). This may account for the marked increase in adsorption which follows addition of HA to PL. Reconstitution studies have previously demonstrated that SP-A, in combination with HA, leads to in vitro formation of tubular myelin, which is not observed in PL samples

containing either HA or SP-A alone (33). The film structure attained by PL + HA + SP-A may specifically be important for achieving high surface pressures during film compression at body temperature under physiological conditions.

Surface-tension measurements made in vitro during large surface-area excursions (i.e., $\Delta A/A_{mean} > 50\%$ by using a Wilhelmy balance or pulsating-bubble surfactometer) allow low minimum surface tensions to be achieved even for films with adsorption kinetics and isotherm properties markedly different from those of CLS. The potential in vivo biophysical consequences of such differences may not become evident until area excursions that more closely approximate those of tidal breathing ($\Delta A/A_{mean} \approx 20\%$) are considered. Figure 9 shows computer simulations for our baseline case of CLS during tidal breathing at area excursions of 20% and how the baseline would be altered by a 50% reduction of m_2. Simulations for CLS samples reach γ_{min} of 1 dyn/cm, whereas those with a lowered value of m_2 reach only 11 dyn/cm. These simulated results are very similar to data obtained for CLS at this smaller area excursion and to those observed for samples containing PL + HA which do, indeed, function as if they have a lower m_2 value as a consequence of the lack of SP-A. (The model does not capture the hysteresis of the PL + HA, presumably because film rupture has not been modeled, as has been previously mentioned). These results reflect the importance of m_2, and presumably SP-A, during dynamic cycling at small area excursions and the potential importance of SP-A during normal respiration.

To stabilize alveolar structures at functional residual capacity during tidal breathing, lung surfactant must possess several critical biophysical properties (16). *1*) It must achieve low surface tensions during film compression over the frequency and amplitude range consistent with tidal breathing. *2*) It must do so under steady-state conditions during repeated cycling; this implies the ability to adsorb to the air-liquid interface after extrusion into the surfactant subphase with a characteristic time similar to or less than the period over which respiration occurs. The present study demonstrates that a minimum of three surfactant constituents are required to impart this behavior: surfactant PLs, HAs, and SP-A. Each biochemical component contributes specific biophysical properties to surfactant; thus a mixture of PL + 3% (by weight) HA + 5% (by weight) SP-A functions nearly the same as native calf surfactant at all frequencies, amplitudes of oscillation, and bulk phase concentration that we examined. Of course, we must here acknowledge a major limitation of these results; namely, these experiments were done in vitro, and detailed confirmation of these conclusions would need to be done in whole lungs.

Although SP-A has recently been shown to play an important immunological function in the lung (20), the results reported here, in conjunction with previous studies (9, 27), argue that SP-A, in combination with PL and HA, is important for determining surfactant dynamic function. Whereas SP-A-deficient organic extracts have previously been shown to improve function in surfactant-deficient animal models with decreased lung compliance, many of these measurements were, in fact, made under quasi-static conditions or at large volume excursions, which would tend to mask the effects of SP-A deficiency. Furthermore, it has been shown that as little as 1% SP-A by weight can have a beneficial effect on the function of organic extracts of lung surfactant (25). Thus animal models in which SP-A-deficient organic extracts have been shown to restore normal or near normal function may contain residual SP-A in sufficient amounts to be biophysically active. The commercial calf lung organic extract Survanta, which is clinically effective as a biologically active lung surfactant, is supplemented with DPPC and palmitic acid such that it functions similarly to CLS at concentrations of 1 mg/ml or greater (22). Thus, although Survanta contains no SP-A, the additional lipid components impart to the PL + HA mixture biophysical properties that approximate those imparted by SP-A.

In summary, our results indicate that individual surfactant constituents have specific effects on the dynamic interfacial behavior of lung surfactant. The HAs had two important effects on dynamic behavior. *1*) Their addition increased the adsorption rate of PL 100-fold. *2*) They stabilized the surface film during compression to allow for $\gamma_{min} < 1$ dyn/cm rather than γ_{min} of ~20 dyn/cm as noted in PL alone. Addition of SP-A restored dynamic film behavior further toward that of CLS; this resulted in an increase in the slope relating surface concentration to surface tension during film compression (m_2). In the presence of SP-A, the NL did not appear to further influence steady-state dynamic film behavior. These studies suggest that native surfactant requires both HA and SP-A to function normally in the human lung, whereas the NL components do not appear to be important in determining function when both HA and SP-A are present.

This work was supported by National Heart, Lung, and Blood Institute Grant P01-HL-33009 and by a National Science Foundation Fellowship to J. Morris.

Address for reprint requests and other correspondence: E. P. Ingenito, Brigham and Women's Hospital, 75 Francis St. Boston, MA 02115 (E-mail: epingenito@bics.bwh.harvard.edu).

Received 1 July 1998; accepted in final form 7 January 1999.

REFERENCES

1. **Ames, B. N.** Assay of inorganic phosphate, total phosphate, and phosphatases. *Meth. Enzymol.* 8: 115–118, 1966.
2. **Chang, D. H., and E. I. Franses.** Dynamic tension behavior of aqueous octanol solutions under constant-area and pulsating-area conditions. *Chem. Eng. Sci.* 49: 313–325, 1994.
3. **Cochrane, C. G., and S. D. Revak.** Pulmonary surfactant protein B: structure function relationships. *Science* 254: 566–568, 1991.
4. **Egberts, J., H. Sloat, and A. Mazure.** Minimal surface tension, squeeze-out and transition temperatures of binary mixtures of dipalmitoylphosphatidylcholine and unsaturated phospholipids. *Biochim. Biophys. Acta* 1002: 109–112, 1989.
5. **Folch, J., M. Lee, and G. H. Sloan-Stanley.** A simple method for isolation and purification of total lipids from animal tissue. *J. Biological Chem.* 226: 497–509, 1957.

6. **Goerke, J., and J. Gonzales.** Temperature dependence of dipalmitoylphosphatidylcholine monolayer stability. *J. Appl. Physiol.* 51: 1108–1114, 1981.
7. **Hall, S. B., Z. Wang, and R. H. Notter.** Separation of subfractions of the hydrophobic components of calf lung surfactant. *J. Lipid Res.* 35: 1386–1394, 1994.
8. **Hawco, M. W., J. P. Davis, and M. W. Keough.** Lipid fluidity in lung surfactant: monolayers of saturated and unsaturated lecithins. *J. Appl. Physiol.* 51: 509–515, 1981.
9. **Hawgood, S., B. J. Benson, J. Schilling, D. Damm, J. A. Clements, and R. T. White.** Nucleotide and amino acid sequences of pulmonary surfactant protein SP 18 and evidence for cooperation between SP 18 and SP 28–36 in surfactant lipid adsorption. *Proc. Natl. Acad. Sci. USA* 84: 66–70, 1987.
10. **Hildebran, J. N., J. Goerke, and J. A. Clements.** Pulmonary surface film stability and composition. *J. Appl. Physiol.* 47: 604–611, 1979.
11. **Johnson, D. O., and K. J. Stebe.** Oscillating bubble tensiometry: a method for measuring the surfactant adsorptive-desorptive kinetics and the surface dilational viscosity. *J. Colloid Interface Sci.* 168: 21–31, 1994.
12. **Kaplan, R. S., and P. L. Pederson.** Determination of microgram quantities of protein in the presence of milligram levels of lipid with amido black 10B. *Analyt. Biochim.* 150: 97–104, 1985.
13. **Kates, M.** Separation of lipid mixtures In: *Techniques of Lipidology: Isolation, Analysis and Identification of Lipids*. London: Elsevier, 1986, p. 186–276.
14. **Mangold, H. K.** *Thin Layer Chromatography*, edited by E. Stahl. New York: Springer, 1969, p. 363–421.
15. **Morris, J.** *Characterization of the Dynamic Behavior of Lung Surfactant and Its Components* (Master's thesis). Cambridge, MA: Massachusetts Institute of Technology, 1998.
16. **Notter, R. H.** Biophysical behavior of lung surfactant: implications for respiratory physiology and pathophysiology. *Semin. Perinatol.* 12: 180–212, 1988.
17. **Notter, R. H., and P. E. Marrow.** Pulmonary surfactant: a surface chemistry viewpoint. *Ann. Biomed. Eng.* 3: 119–159, 1975.
18. **Notter, R. H., R. Taubold, and R. D. Mabis.** Hysteresis in saturated phospholipid films and its potential relevance for lung surfactant function in vivo. *Exp. Lung Res.* 3: 109–127, 1982.
19. **Otis, D. R., Jr., E. P. Ingenito, R. D. Kamm, and M. Johnson.** Dynamic surface tension of surfactant TA: experiments and theory. *J. Appl. Physiol.* 77: 2681–2688, 1994.
20. **Possmayer, F.** The role of surfactant-associated proteins. *Am. Rev. Respir. Dis.* 142: 749–752, 1990.
21. **Poulain, F. R., L. Allen, M. C. Williams, R. L. Hamilton, and S. Hawgood.** Effects of surfactant apolipoproteins on liposomal structure: implications for tubular myelin formation. *Am. J. Physiol.* 262 (*Lung Cell. Mol. Physiol.* 6): L730–L739, 1992.
22. **Putz, G., J. Goerke, H. W. Taeusch, and J. A. Clements.** Comparison of captive and pulsating bubble surfactometers with use of lung surfactants. *J. Appl. Physiol.* 76: 1425–1431, 1994.
23. **Rana, F. R., A. J. Mautone, and R. A. Dluhy.** Surface chemistry of binary mixtures of phospholipids in monolayers. Infrared studies of surface composition at varying surface pressures in a pulmonary surfactant model system. *Biochemistry* 32: 3169–3177, 1993.
24. **Revak, S. D., T. A. Merritt, E. Degryse, L. Stefani, M. Courtney, M. Hallman, and C. G. Cochrane.** Use of human surfactant low molecular weight apoproteins in the reconstitution of surfactant biological activity. *J. Clin. Invest.* 81: 826–833, 1988.
25. **Schürch, S., F. Possmayer, S. Cheng, and A. M. Cockshutt.** Pulmonary SP-A enhances adsorption and appears to induce surface sorting of lipid extract surfactant. *Am. J. Physiol.* 263 (*Lung Cell. Mol. Physiol.* 7): L210–L218, 1992.
26. **Searcy, R. L., and L. M. Bergquist.** A new color reaction for the quantitation of serum cholesterol. *Clin. Chim. Acta* 5: 192–199, 1960.
27. **Suzuki, Y.** Effect of protein, cholesterol, and phosphatidylglycerol on the surface activity of the lipid-protein complex reconstituted from pig pulmonary surfactant. *J. Lipid Res.* 23: 62–69, 1982.
28. **Suzuki, Y., E. Nakai, and K. Ohkawa.** Experimental studies on the pulmonary surfactant. Reconstitution of surface active material. *J. Lipid Res.* 23: 53–61, 1982.
29. **Tanford, C.** *The Hydrophobic Effect: Formation of Micelles and Biological Membranes.* New York: Wiley, 1980, p. 94–111.
30. **Tchoreloff, P., A. Gulik, B. Denizot, J. E. Proust, and F. Puisieux.** A structural study of interfacial phospholipid and lung surfactant layers by transmission electron microscopy after Blodgett sampling: influence of surface pressure and temperature. *Chem. Phys. Lipids* 59: 151–165, 1991.
31. **Touchstone, J. C., J. C. Chen, and K. M. Veaver.** Improved separation of phospholipids in thin layer chromatography. *Lipids* 15: 61–62, 1980.
32. **Wang, Z., S. B. Hall, and R. H. Notter.** Dynamic surface activity of films of lung surfactant phospholipids, hydrophobic proteins, and neutral lipids. *J. Lipid Res.* 36: 1283–1293, 1995.
33. **Williams, M. C., S. Hawgood, and R. L. Hamilton.** Changes in lipid strucutre produced by surfactant proteins SP-A, SP-B, SP-C. *Am. J. Respir. Cell Mol. Biol.* 5: 41–50, 1991.